Polyhedron 88 (2015) 73–80

Contents lists available at ScienceDirect

Polyhedron

journal homepage: www.elsevier.com/locate/poly

Photophysical and non-linear optical behavior of novel tetra alkynyl terminated indium phthalocyanines: Effects of the carbon chain length

Owolabi M. Bankole, Jonathan Britton, Tebello Nyokong *

Department of Chemistry, Rhodes University, Grahamstown 6140, South Africa

A R T I C L E I N F O

Article history:
Received 4 November 2014
Accepted 20 December 2014
Available online 30 December 2014

Keywords:
Nonlinear optical absorption
Alkynyl indium phthalocyanine
Hyperpolarizability
Third order susceptibility
Reverse saturable absorption

A B S T R A C T

We report on the synthesis, photophysical and nonlinear optical behavior of tetra-substituted alkynyl indium phthalocyanine complexes (**3a** and **3b**). Both complexes showed large triplet quantum yields. Nonlinear optical properties were also evaluated for the two complexes at a wavelength of 532 nm using nanosecond Z-scan technique in dimethylsulfoxide. We observed two-photon absorption (2PA) and strong reverse saturable absorption (RSA) as the dominant mechanisms at nanosecond laser excitation. The underlining 2PA and observed RSA were subjected to further scrutiny by comparing the analytical absorption model to the transmittance optical absorption theory. The theoretical results were in good agreement to the observed RSA and the 2PA mechanism. Large two-photon absorption cross-section (1.29×10^{-42} and 1.15×10^{-42} cm^4 s/photon), third-order susceptibility (2.10×10^{-14} and 2.15×10^{-14} esu) and hyperpolarizability (2.70×10^{-32} and 3.19×10^{-32} esu) were estimated for complex **3a** and **3b**, respectively.

1. Introduction

Phthalocyanines (Pcs) have been used for a diverse range of applications including in liquid crystals, photodynamic therapy (PDT), Langmuir–Blodgett films, chemical sensors, semiconductors, electrochromic devices, ink-jet printing, electrophotography and electrocatalysis [1–8]. The aforementioned applications rely on the Pcs' degree of aromaticity, unique electronic properties, high thermal- and photo-stability and the architectural flexibility [9].

One of the emerging applications of these molecules as discussed in this work is their use as potential nonlinear optical limiters [10–13]. The application of phthalocyanines as potential nonlinear optical (NLO) materials is partly based on the mechanism known as reverse saturable absorption (RSA) [14–18]. The other mechanism responsible is two-photon absorption. NLO materials protect sensors and human eyes from laser radiation by effectively limiting the energy output of an incident light [19,20]. Modifications of phthalocyanine structures for improved optical limiting purposes include the use of a variety of central metal atoms, axial ligands and/or peripheral substituents [21].

Intense investigation into photophysical behavior of indium, gallium and lead phthalocyanine derivatives as potential nonlinear optical materials, have been carried out [22–24]. This paper describes for the first time, the synthesis, photophysical studies and nonlinear properties of indium phthalocyanines functionalized with alkynyl-containing moieties at the peripheral positions of the phthalocyanine ring. The rationale behind this novel idea as contained in this research is based on: (1) the use of heavy metal atom at the centre of the phthalocyanines and (2) presence of chromophore containing an acetylene unit.

Indium is used as the central metal to increase the rate of intersystem crossing via spin–orbit coupling and also to increase the hyperpolarizability of the phthalocyanines [25]. The axial ligation (Cl used in this case) minimizes intermolecular interactions which cause aggregation of phthalocyanines in solution [26]. It has been reported that the Introduction of groups containing triple bonds enhances the intersystem crossing rate [27], hence we employed these groups in this work.

To the best of our knowledge, placing terminal alkynyl moieties on the peripheral positions of indium phthalocyanines has not been reported before. Thus, we report for the first time the synthesis, characterization and nonlinear optical properties of In-phthalocyanine tetra-substituted 5-hexyl-1-ol and 2-propyl-1-ol on the peripheral positions, Scheme 1. The effect of the chain length is assessed. NLO behavior of alkynyl substituted phthalocyanines have been reported for complexes containing Zn and Co [28] and with no spacer between the terminal group and the Pc ring. Low values of hyperpolarizability were obtained [28]. In this work, spacers are placed between the Pc ring and the terminal alkynyl group, with improved hyperpolarizability. The presence of the alkynyl group allows for future modification of the molecules using click chemistry.

---

* Corresponding author. Tel.: +27 46 6038260; fax: +27 46 6225109.
E-mail address: t.nyokong@ru.ac.za (T. Nyokong).

http://dx.doi.org/10.1016/j.poly.2014.12.020
0277-5387/

The optical limiting behavior of phthalocyanines molecules have been assessed by using different techniques including transient absorption and Z-scan methods [29] and third harmonic generation (THG) [30]. The nonlinear behavior of the synthesized complexes are measured using the Z-scan in this work.

2. Experimental

2.1. Materials

5-Hexy-1-ol, propargyl alcohol, dichloromethane (DCM), 4-nitrophthalonitrile, 1,8-diazabicyclo[5.4.0]undec-7-ene (DBU), zinc phthalocyanine (ZnPc), *n*-pentanol, diethylether, potassium carbonate and indium (III) chloride were obtained from Sigma Aldrich. Deuterated dimethyl sulfoxide (DMSO-d_6), *n*-hexane, methanol, dimethyl formamide (DMF) and dimethyl sulfoxide (DMSO) were purchased from Merck. All solvents were of reagent grade and were freshly distilled before use. The progress of the syntheses was monitored using SiO_2 thin layer chromatography (TLC).

2.2. Equipment and methods

Infra-red spectra were collected on a Perkin-Elmer Universal ATR Sampling accessory spectrum 100 FT-IR spectrometer. ^{1}H NMR spectra were obtained using a Bruker AVANCE 400 MHz NMR spectrometer in DMSO-d_6. Elemental analyses were done using a Vario-Elementar Microcube ELIII, while mass spectra data were collected on a Bruker AutoFLEX III Smart-beam TOF/TOF mass spectrometer using α-cyano-4-hydrocinnamic acid as the matrix in the positive ion mode.

Ground state electronic absorption spectra were recorded on a Shimadzu UV-2550 spectrophotometer. Fluorescence emission spectra were recorded on a Varian Eclipse spectrofluorimeter. Time Correlated Single Photon Counting (TCSPC) setup (FluoTime 200, Picoquant GmbH) was used for the fluorescence decay studies. The excitation source was a diode laser (LDH-P-670 driven by PDL 800-B, 670 nm, 20 MHz repetition rate, 44 ps pulse width, Picoquant GmbH).

All Z-scan analyses were performed using a frequency-doubled Nd:YAG laser (Quanta-Ray, 1.5 J/10 ns fwhm pulse duration) as the excitation source. The laser was operated in a near Gaussian transverse mode at 532 nm (second harmonic), with a pulse repetition rate of 10 Hz and energy range of 0.1 μJ–0.1 mJ, as limited by the energy detectors (Coherent J5-09). The low repetition rate of the laser prevents cumulative thermal nonlinearities. The beam was spatially filtered to remove the higher order modes and tightly focused with a 15 cm focal length lens. The Z-scan system size (l × w × h) used was 600 mm × 300 mm × 350 mm (excluding the computer, energy meter, translation stage driver and laser system). The liquid samples were placed in a cuvette (internal dimensions: 2 mm × 10 mm × 55 mm, 0.7 mL) and a path length of 2 mm (Starna 21-G-2).

The nanosecond flash photolysis set-up to investigate the triplet state behavior comprised of coupled laser systems, a Nd-YAG laser (already described above) pumping Lambda-Physik FL3002 dye (Pyridin 1 dye in methanol) laser. The analyzing beam source was a Thermo Oriel 66902 xenon arc lamp. Details have been provided before [22].

2.3. Synthesis

2.3.1. 4-Hexy-5-ynyloxy-phthalonitrile (**2a**) (Scheme 1)

4-Nitrophthalonitrile (**1**) (2 g, 11.5 mmol) was dissolved in dry DMSO (20 mL) and 5-hexyn-1-ol (1.69 g, 11.5 mmol) added under a nitrogen atmosphere. After stirring for 10 min, finely ground anhydrous K_2CO_3 (2.16 g, 15.6 mmol) was added in portions over 2 h, with stirring. The reaction mixture was stirred at 40 °C for 48 h under nitrogen. Then the mixture was poured into 400 mL of cold water. The precipitate was filtered off and washed with water, until the filtrate was neutral. Recrystalization from hexane and methanol gives the desired compound as a yellow crystalline powder. Yield: 1.74 g (60%). IR (KBr) ν_{max}/cm^{-1}: 3282 ($\equiv$C—H); 2228 (CN); 2222 ($C\equiv C$); 1557, 1488 (C=C phenyl); 1287 (Ar–O–C); 1308 1251, 1003, 840, 660. *Anal.* Calc. for $C_{14}H_{12}N_2O$: C, 74.98; H, 5.39; N, 12.49. Found: C, 74.56; H, 5.23; N, 12.36%. ^{1}H NMR (600 MHz, DMSO-d_6): δ, ppm: 8.02 (Ar-H, s, 1H), 7.75 (Ar-H, d, 1H), 7.43 (Ar-H, d, 1H), 4.15 (CH_2–O–, t, 2H), 2.77 ($C\equiv CH$, s, 1H), 2.22 (CH_2, t, 2H), 1.81 (CH_2, m, 2H), 1.58 (CH_2, m, 2H).

2.3.2. 4-Propy-2-ynyloxy-phthalonitrile (**2b**) (Scheme 1)

Compound **2b**, Scheme 1, was synthesized following the method described above for compound **2a**, using propargyl alcohol (b) (0.64 g, 11.5 mmol) in place of 5-hexyn-1-ol. Yield: 1.42 g (75%). IR (KBr) ν_{max}/cm^{-1}: 3286 ($\equiv$C—H); 2229 (CN); 2222 ($C\equiv C$); 1557, 1488 (C=C phenyl); 1288 (Ar–O–C); 1306, 1256, 1011, 829, 670. *Anal.* Calc. for $C_{11}H_6N_2O$: C, 72.52; H, 3.32; N, 15.38. Found: C, 71.77; H, 3.14; N, 15.19%. ^{1}H NMR (600 MHz, DMSO-d_6): δ, ppm: 8.09 (Ar-H, d, 1H), 7.80 (Ar-H, d, 1H), 7.49 (Ar-H, dd, 1H), 5.00 (CH_2–O–, t, 2H), 3.70 ($C\equiv CH$, s, 1H).

2.3.3. 2,9(10),16(17),23(24)-Tetrakis(hex-5-ynoxy)phthalocyanatoindium(III) chloride (**3a**) (Scheme 1)

A mixture of 4-hexy-5-ynyloxy-phthalonitrile (**2a**) (0.25 g, 1.11 mmol), indium (III) chloride (0.25 g, 1.11 mmol) and few drops of catalytic DBU in *n*-pentanol (1.5 mL) was stirred under reflux at 140 °C for 20 h. The reaction was carried out under argon. The crude dark blue product was cooled to room temperature and washed with methanol, ethanol, 1 M HCl and acetone in succes-

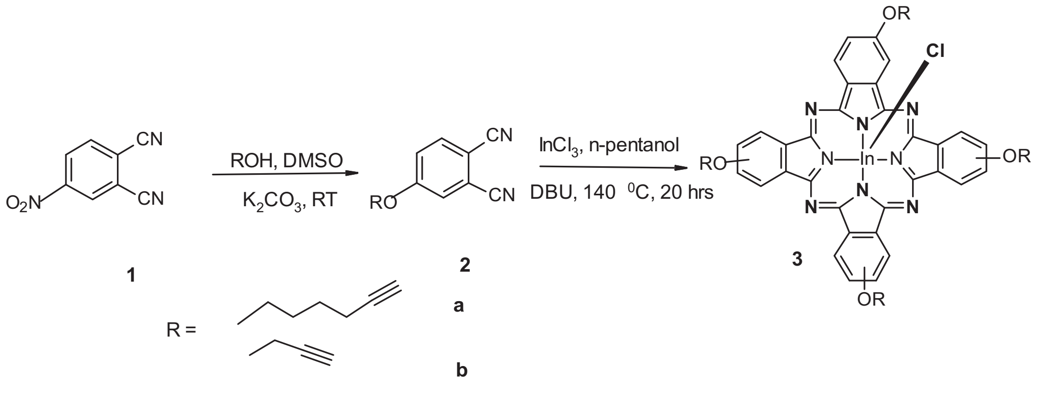

Scheme 1. Synthetic pathway for complexes **3a** and **3b**.

sion. Further purification of the compound was achieved by Soxhlet extraction using ethanol–water (1:1) for 24 h to remove the traces of DBU from the compound. Column chromatography on silica gel as stationary phase and tetrahydrofuran (THF):methanol as eluent was also performed. The blue-green indium phthalocyanine obtained was thereafter concentrated and dried.

Yield: 64.6%, UV–Vis (DMSO): λ_{max}/nm (log ε): 696 (5.07), 629 (4.40), 358 (4.83). FT-IR [KBr disc (ν_{max}/cm^{-1})]: 3285 ($\equiv$C-H); 2934 (CH aliphatic); 3089 (Ar-H); 2222 (C$\equiv$C); 1228, 1118, 1081, 1045 (C–O–C), 966, 824, 741, 650 (Pc-Skeleton). *Anal.* Calc. for $C_{56}H_{48}N_8O_4InCl.H_2O$: C, 63.31; H, 4.70; N, 10.52. Found: C, 63.26; H, 4.91; N, 10.68%. MS (MALDI-TOF) *m/z*: Calcd. 1046.36; Found: 1049.22 [M+3H]$^+$. ^{1}H NMR (600 MHz, DMSO-d_6): δ, ppm:8.53 (Ar-H, d, 4H), 7.62 (Ar-H, s, 4H), 7.18 (Ar-H, dd, 4H), 4.09 (CH$_2$–O–, t, 8H), 2.11 (C$\equiv$CH, s, 4H), 1.75 (CH$_2$, m, 8H), 1.48 (CH$_2$, m, 8H), 1.09 (CH$_2$, t, 8H).

2.3.4. 2,9(10),16(17),23(24)-Tetrakis(prop-2-ynoxy)phthalocyanatoindium(III) chloride (3b) (Scheme 1)

A mixture of 4-propy-2-ynyloxy-phthalonitrile (**2b**) (0.3 g, 1.64 mmol), indium (III) chloride (0.36 g, 1.64 mmol) and 20 μl of catalytic DBU in *n*-pentanol (1.7 mL) was heated to 140 °C under nitrogen for 20 h. The crude dark product was cooled to room temperature and washed with methanol, ethanol, 1 M HCl and acetone in succession. Further purification of the compound was achieved only by Soxhlet extraction using ethanol–water (1:1) for 24 h to remove the traces of DBU from the compound. The blue-green indium phthalocyanine obtained was thereafter concentrated and dried.

Complex **3b** yield: (75%). UV–Vis (DMSO): λ_{max}/nm (log ε): 693 (5.01), 625 (4.35), 360 (4.75). FT-IR [KBr disc (ν_{max}/cm^{-1})]: 3286 ($\equiv$C—H); 2929 (CH aliphatic); 3077 (Ar-H); 2161 (C$\equiv$C); 1604 (Ar C–C), 1280, 1215, 1084, 1011 (C–O–C), 939, 825, 742, (Pc-Skeleton). *Anal.* Calc. for $C_{44}H_{24}N_8O_4InCl$: C, 60.12; H, 2.75; N, 12.75. Found: C, 60.01; H, 2.74; N, 12.01%. MS (MALDI-TOF) *m/z*: Calcd. 878.86; Found: 879.36 [M+H]$^+$. ^{1}H NMR (600 MHz, DMSO-d_6): δ, ppm: 8.44 (Ar-H, d, 4H), 7.78 (Ar-H, s, 4H), 7.36 (Ar-H, dd, 4H), 4.45 (CH$_2$–O–, t, 8H), 2.70 (C$\equiv$CH, s, 4H).

2.4. Fluorescence and triplet quantum yields

Fluorescence (Φ_F) and triplet (Φ_T) quantum yields were determined using established methods [31–33] using ZnPc as a standard in DMSO ($\Phi_F = 0.2$ [33] and $\Phi_T = 0.65$) [32].

Quantum yields of internal conversion (Φ_{IC}) were obtained from Eq. (1), which assumes that fluorescence, intersystem crossing and internal conversion are the only three processes which are jointly responsible for the deactivation of the excited singlet state of both indium (III) phthalocyanine molecules (**3a** and **3b**):

$$\Phi_{IC} = 1 - (\Phi_F + \Phi_T) \tag{1}$$

The triplet lifetimes were determined by fitting the data obtained to single exponential using OriginPro 8 program.

2.5. Nonlinear optical parameters

The nonlinear optical properties of phthalocyanines are evaluated using the Z-scan technique that has been previously described [34,35]. The technique relies on the total transmittance passing through the sample as a result of the incident laser pulses. The general equation for normalized transmittance ($T_{norm(Z)}$) can be written as Eq. (2).

$$T_{norm(Z)} = \frac{1}{1 + \beta_2 L_{eff}(I_{00}/(1 + (z/z_0)^2))} \tag{2}$$

where I_{00} is the intensity of the light on focus, β_2 is the two photon absorption (2PA) coefficient, L_{eff}, z and z_0 are the effective path length in the sample of length L, translation distance of the sample relative to the focus and Rayleigh length, respectively. Rayleigh length is defined as $\pi w_o^2/\lambda$, where λ is the wavelength of the laser and w_o is the beam waist at the focus, ($z = 0$). L_{eff} is given by Eq. (3):

$$L_{eff} = \frac{1 - e^{-\alpha L}}{\alpha} \tag{3}$$

where α is the linear absorption coefficient.

The molecular two-photon absorption (MTPA) cross-section σ_2 (cm^4 s/photon) can be calculated from the known two-photon absorption coefficient (β_2) using Eq. (4) [36]:

$$\sigma_2 = \frac{1000 h\upsilon\beta_2}{N_A C} \tag{4}$$

where, $h\upsilon$ is the incident photon measured in joules, N_A is the Avogadro constant, C is the concentration of the sample.

The imaginary third-order susceptibility ($I_m[\chi^{(3)}]$) is directly proportional to the two-photon absorption coefficient, β_2 as shown in Eq. (5) [37]:

$$I_m[\chi^{(3)}] = n^2 \varepsilon_0 c \lambda \beta_2 / 2\pi \tag{5}$$

where, n is the linear refractive index, c is the speed of light respectively, ε_0 is the permittivity of free space and λ is the wavelength of the laser.

The relationship between second order hyperpolarizability (γ) and third-order susceptibility ($I_m[\chi^{(3)}]$) of the material is given by Eq. (6) [12]:

$$\gamma = \frac{I_m[\chi^{(3)}]}{f^4 C_{mol} N_A} \tag{6}$$

where C_{mol} is the molar concentration of the active species in the triplet state, f is the Lorentz local field enhancement factor, defined as $f = (n^2 + 2)/3$; n is the refractive index of the sample and N_A as defined above.

3. Results and discussion

3.1. Synthesis and characterization

The novel In-phthalocyanines (**3a** and **3b**) containing terminal alkyne at the peripheral positions Pcs are reported for the first time in this work.

Modification of phthalocyanine molecules to further improve their architectural flexibility with terminal alkynes is now becoming an active area of research [38–41]. The compounds are readily soluble in organic solvents such as DMF, DCM, THF, chloroform and DMSO. The alkyne chain-length of compounds **3a** and **3b** were carefully chosen to determine the effect of the chain length on both the photophysical and non-linear optical properties of the new phthalocyanines.

Targeted alkynyl-phthalonitriles (**2a** and **2b**) were synthesized via a based-catalyzed nucleophilic aromatic displacement between 4-nitrophthalonitrile (**1**) and propargyl alcohol and 5-hexy-1ol, Scheme 1. Cyclotetramerization of **2a** and **2b** (to form **3a** and **3b**) occurred in the presence of the desired metal salt ($InCl_3$) and a catalytic amount of DBU. Since a large atom like indium requires high energy to insert the metal ion into the phthalocyanine cavity, high-boiling solvent, *n*-pentanol, was employed in order to obtain the desired complexes, **3a** and **3b** [42]. The compounds were obtained in satisfactorily high yields and were characterized by elemental analysis, UV–Vis, FT-IR, ^{1}H NMR spectroscopies and MALDI-TOF. The characterization results are consistent with the predicted structures as shown in the experimental section. The elemental analyses gave percentage carbon values that were within 1% in all cases, which are within acceptable range for phthalocyanine complexes.

In both cases a mixture of four possible structural isomers are obtained for tetra-substituted phthalocyanines. The four probable isomers can be designed by their molecular symmetry as C_{4h}, C_{2v}, C_s and D_{2h} [43]. In this study, synthesized tetra-substituted phthalocyanine compounds are obtained as isomer mixtures as expected. No attempt was made to separate the isomers for **3a** or **3b**.

After conversion of the substituted phthalonitriles to indium phthalocyanines (**3a** and **3b**), the characteristics intense IR peak (Fig. 1) around 2230 cm^{-1}, which is associated with C$\equiv$N stretch in phthalonitriles, disappeared to confirm the formation of metallo-phthalocyanine complexes. Other notable signals at 3285 and 3286 cm^{-1} are due to C$\equiv$C—H, for **3a** and **3b**, respectively. The complexes showed characteristic vibrations due to ether groups (C–O–C) 1011–1279 cm^{-1}, aromatic CH stretching at ca. 3076 cm^{-1} and aliphatic CH stretching at ca. 2928–2934 cm^{-1}.

The mass spectral studies on the newly synthesized phthalocyanines was definitive and gave expected masses of the complexes **3a** and **3b**. The observed molecular ion peaks for complex **3a** was found at m/z = 1049.22 which is attributed to $[M+3H]^+$ and m/z = 879.36 $[M+H]^+$ for **3b**. Fragmentation of molecular ion peaks as $[M]^+$, $[M+nH]^+$, or $[M-nH]^-$ have been reported [44], hence the observed mass spectral pattern for **3a**. The mass and ^{1}H NMR spectra and the elemental analysis confirm the purity of the synthesized complexes.

3.2. Ground state electronic absorption and fluorescence spectra

The Q-bands for **3a** and **3b** (Fig. 2) in DMSO were observed at 696 nm (**3a**) and 693 (**3b**) (Table 1). Alkyne substituted phthalocyanines are known for metal free or metals such as Zn and Co [45], with not much change in the Q band with change in central metal. The Q-band of complex **3a** was red-shifted by 3 nm, compared to **3b**. This red shift is due to increase in carbon chain-length for 5-hexy-1-ol (**3a**) which shifts the peak to a slightly longer wavelength due to the interaction between σ bonded electrons of the alkynyl group and the π bond electrons in the triple bonds [46]. This leads to slight destabilization of highest occupied molecular orbital (HOMO) level in **3a** and result in the shift to the longer wavelength [46]. Both complexes **3a** and **3b** show red-shifted Q band when compared to unsubstituted InPc [47], Table 1. This could be due to the electron donating abilities of alkynyl groups. Electron donating groups are known to result in the red shifting of the Q band [48].

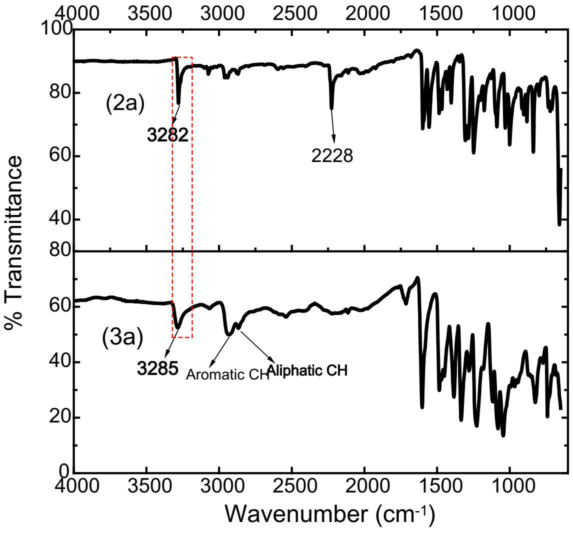

Fig. 1. FT-IR spectra of **2a** and **3a**.

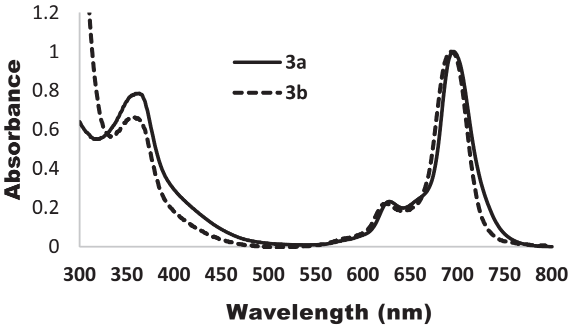

Fig. 2. Absorption spectra of **3a** (solid line) and **3b** (dotted line) in DMSO.

Fluorescence behavior of the synthesized ClInPc derivatives (**3a** and **3b**) in DMSO were similar to each other. Fluorescence is weak for both complexes due to the heavy atom effect of In, Fig. 3. The excitation spectra was slightly red-shifted compared to the absorption spectra for both complexes. Also the excitation spectrum was broad compared to absorption spectra. This indicates change in nuclear configuration following excitation. The loss of symmetry is possible due to the large size of indium metal which is more displaced from the cavity of the phthalocyanines ring and become more pronounced upon excitation [49]. The Stokes shifts are small as typical of phthalocyanines [47].

The aggregation behavior of the synthesized phthalocyanines was investigated using absorption studies in DMSO at different concentrations. As the concentration was increased, the intensity of the absorption of the Q-band also increased without formation of new bands due to the aggregated species for both complexes (**3a** and **3b**) [50]. The Beer–Lambert law was obeyed for both complexes in DMSO in the concentrations ranging from 1.8×10^{-6} to 3.0×10^{-6} M.

3.3. Photophysical studies

3.3.1. Fluorescence lifetimes and quantum yields

The fluorescence quantum yields (Φ_F) for **3a** and **3b** were consistent with MPc complexes containing heavy metals. The values obtained are lower than that of unsubstituted ClInPc ($\Phi_F = 0.018$ [47], Table 1, suggesting quenching of fluorescence by alkynyl groups. Compound **3a** has a larger Φ_F value, this suggest less fluorescence quenching of the excited singlet state in **3a** compared to **3b**.

The fluorescence lifetimes (τ_F) for the compounds were obtained from TCSPC technique by fitting the fluorescence decay data to a bi-exponential function (Fig. 4). The presence of two lifetimes for phthalocyanines may be attributed to the presence of aggregates which quench fluorescence to give quenched (shorter) and unquenched (longer) lifetimes [51]. The average lifetimes (τ_{avF}) reported for the compounds are within the range of reported values of phthalocyanines [52]. τ_{avF} values for both compounds **3a** and **3b** are low compared to the unsubstituted indium phthalocyanines [47]. Again, this suggests quenching of fluorescence by the alkynyl substituents.

The fluorescence rate constant (k_F) is directly proportional to the fluorescence quantum yield (Φ_F) of the Pcs. Complex **3b** has relatively lower k_F than **3a**, this suggests more quenching in **3b** than **3a** as observed for Φ_F values. The larger rate constant for intersystem crossing (k_{ISC}) for complexes **3a** and **3b** than unsubstituted ClInPc, Table 1, suggest that the presence of alkynyl moieties on the peripheral positions encourages rate of intersystem crossing

Table 1
Spectral and photophysical data for complexes **3a** and **3b** in DMSO.

Complex	${}^{a}\lambda_{abs}$ nm, (log ε)	${}^{a}\lambda_{em}$ nm	${}^{a}\lambda_{exc}$ nm	Φ_F	${}^{b}\tau_F$ (ns)	τ_{avF} (ns)	τ_T (μs)	Φ_T	$\tau_{ISC(av)}$ (ns)	$k_F{}^{c}$ (s^{-1}) (10^7)	$k_{ISC}{}^{d}$ (s^{-1}) (10^9)
3a	696 (5.01)	710	702	0.012	$0.31 \pm 4.0 \times 10^{-3}$ (97.57%) $2.85 \pm 8.0 \times 10^{-2}$ (2.43%)	0.37 ± 0.04	75 ± 0.9	0.82	0.45 ± 0.11	3.2 ± 0.1	2.22 ± 0.11
3b	693 (5.07)	710	706	0.009	$0.32 \pm 4.0 \times 10^{-3}$ (98.39%) $2.72 \pm 13.0 \times 10^{-2}$ (1.61%)	0.36 ± 0.06	66 ± 0.8	0.84	0.43 ± 0.17	2.5 ± 0.2	2.33 ± 0.17
ClInPc	686 (4.46)	700	689	0.018[e]	–	0.90[e]	50[c]	0.91[e]		1.99[e]	1.01[e]

[a] λ_{abs}, λ_{em} and λ_{exc} represent absorbance, emission and excitation wavelengths, respectively.
[b] Abundances in brackets.
[c] $k_F = \Phi_F/\tau_{avF}$, k_F is the fluorescence rate constant.
[d] $k_{ISC} = \Phi_T/\tau_{avF}$, k_{ISC} is the rate constant for intersystem crossing.
[e] Values from Ref. [47].

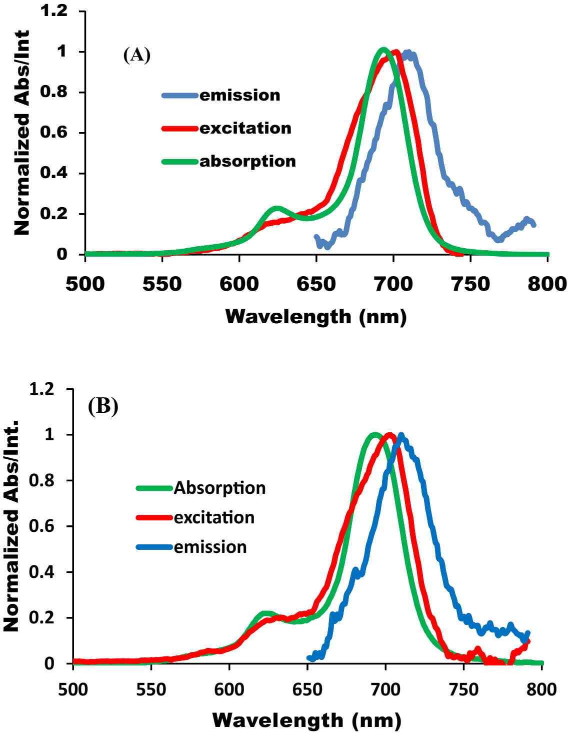

Fig. 3. Absorption, fluorescence emission and excitation spectra of (A) **3a** and (B) **3b** in DMSO. Excitation wavelength = 610 nm.

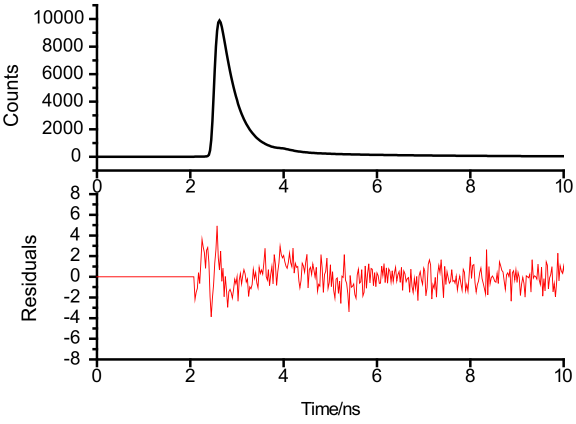

Fig. 4. Fluorescence decay profile of **3a** in DMSO.

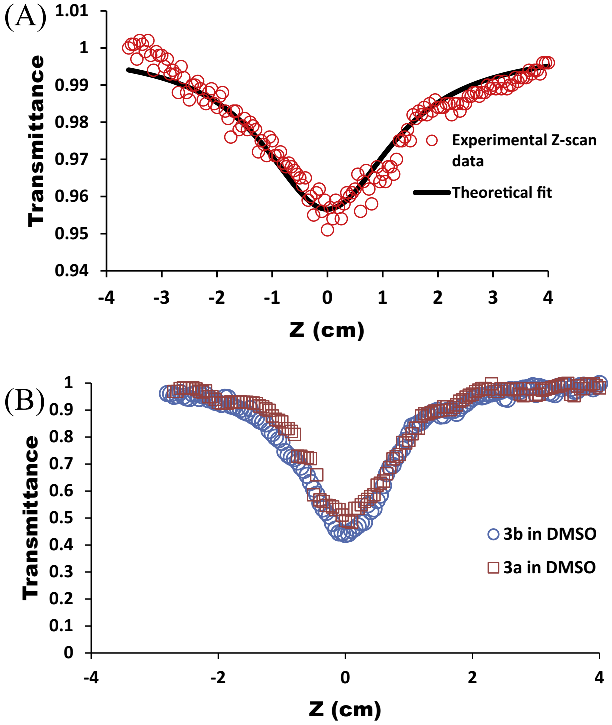

Fig. 5. (A) Open aperture Z-scan for **3b** in DMSO showing the fitting. The black solid curve is the theoretical fit, $I_{00} \approx 60.0$ MW cm^{-2}. (B) Representative open-aperture Z-scans of the compounds **3a** and **3b**. Peak input intensity (I_{00}) ≈ 130 MW cm^{-2}.

from excited singlet to triplet state. The rate of intersystem crossing in complex **3b** is more pronounced than that of **3a**, this can also be attributed to the lower intersystem crossing lifetime observed in compound **3b** compared to **3a**.

3.3.2. Triplet quantum yields and lifetimes

In Table 1, large triplet quantum yields (Φ_T) values are observed for **3a** and **3b** in DMSO due to the presence of heavy atom effect of indium. The triplet lifetimes (τ_T) for the two complexes ranged are low at 66 μs (**3b**) and 75 μs (**3a**), corresponding to the large triplet quantum yields. The values were slightly longer than for unsubstituted InPc, Table 1.

3.4. Nonlinear optical (NLO) studies

3.4.1. Z-scan measurements

Fig. 5(A) shows a representative open aperture Z-scan for complex **3b** recorded at 532 nm and 10 ns pulses using peak input intensity of ca. 60.0 MW cm^{-2}. For irradiance intensities at ca.

Table 2
Nonlinear optical properties of samples **3a** and **3b** in DMSO at 532 nm wavelength and 10 ns pulses. The peak intensity for each measurement was ≈130 MW cm^{-2}.

Complex	β_2 (cm GW^{-1})	$I_m[\chi^{(3)}]$ /esu	γ(esu)	σ_2 (cm^4 s/photon)	k (σ_{ex}/σ_0)	I_{lim} (J cm^{-2})
3a	427	2.10×10^{-14}	2.70×10^{-32}	1.29×10^{-42}	5.17	0.55
3b	438	2.15×10^{-14}	3.19×10^{-32}	1.15×10^{-42}	3.46	0.48

130.0 MW cm^{-2} (Fig. 5B) the normalized transmittance of the two complexes (**3a** and **3b**) dropped below 0.5 making them good optical limiting materials [15,17,53]. The reduction in the linear transmission about the focus of the lens at 532 nm exhibited by each molecule is an indication of positive nonlinear absorption. Such molecules are referred to as exhibiting reverse saturable absorbance (RSA) [15,34,35,53–55] due to the optical limiting possibly being caused by sequential photon absorption. The other mechanism which could be the cause of the optical limiting is two photon absorption (2PA).

The Z-scan data obtained for complexes **3a** and **3b** were found to perfectly fit the transmission equation (Eq. (2)) for two-photon absorption (2PA) function. The estimated nonlinear absorption coefficients (β_2) for **3a** and **3b** are respectively ~ 427 cm GW^{-1} and 438 cm GW^{-1}, Table 2. It is believed that contributions from higher mechanisms such as three-photon absorption (3PA) are also expected for the nonlinearity of the complexes due to the ns pulses and the high peak intensities used [10,15,22,37]. Further analysis to show whether the dominant mechanism for the observed z-scan spectra is from sequential photon reverse saturable absorption or 2PA follows.

3.4.2. Two photon absorption (2PA) and sequential photon (RSA) mechanisms

The Jablonski diagram in Fig. 6, shows the contribution of the excited states of the Pcs to the multi-photon absorption processes observed in the Z-scans [26,56]. 2PA at 532 nm and ns pulsed laser involves simultaneous absorption of two photons by the Pcs through [$S_0 \rightarrow S_n$] transition, followed by the Pc relaxing to the S_1 state, undergoing intersystem crossing to the triplet state and absorbing further singular photons whilst in this state. The RSA mechanism is when the transition to the S_n state occurs with sequential one photon absorption via a virtual level. Once in the S_n state the processes proceed like in the 2PA mechanism. There is also a possibility that there may be relaxation from the virtual level to the S_1 state. The excited state of absorption cross-section (σ_T) being larger than the ground state absorption cross-section (σ_0) is a condition which is primarily responsible for RSA occurring in the Pcs [57–59]. The incident pulses have duration of 10 ns compared to the shorter lifetimes (<1 ns, Table 1, τ_{ISC}) of the Pcs to populate the triplet states T_1 via intersystem system crossing. Also, the high triplet quantum yields of the two compounds (~1) ensure a large ISC to the triplet states as well as [$T_1 \rightarrow T_2$] transitions.

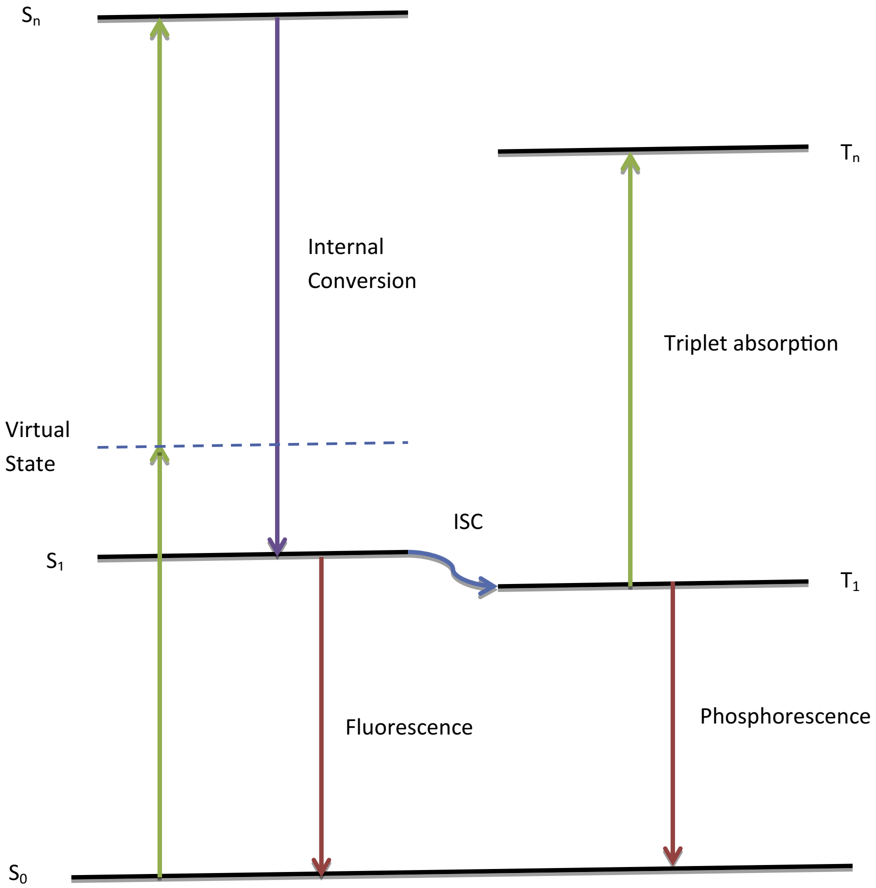

Fig. 6. Jablonski energy level diagram for theorized RSA and/or simultaneous two-photon absorption (2PA) of **3a** and **3b**.

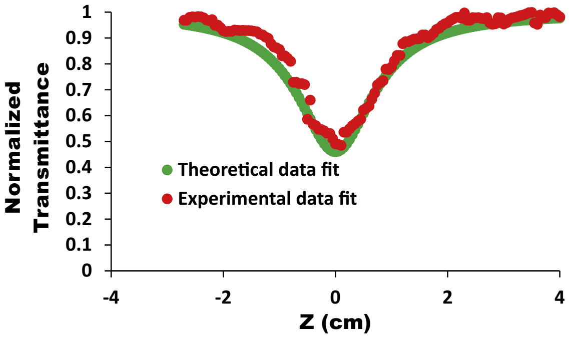

Fig. 7. Representative open aperture (OA) Z-scan fits between experimental data and theoretical analytical of absorption model for complex **3b** in DMSO with varying σ_T parameters.

Analytical absorption model Eq. (7) [60] was used to further verify the existence of 2PA mechanism as opposed to the RSA mechanism for the two complexes.

$$\frac{T}{T_{\text{linear}}} = \frac{\text{In}[1+q]}{q} \tag{7}$$

$$\text{where } q = \frac{\alpha\sigma_T}{2h\upsilon} I_0 L_{\text{eff}} \tag{8}$$

where σ_T is the excited state of absorption cross-section, I_0, L_{eff} and α as defined above.

Theoretical (Fig. 7) OA Z-scan datasets were fitted to the experimental transmittance datasets using least squares regression method while treating σ_T as a free parameter to obtain value of $R^2 \sim 0.9$. The values of σ_T correspond to *T–T* transitions obtained for **3a** and **3b** with the theoretical fits of 8.8×10^{-17} cm^2 and 6.8×10^{-17} cm^2, respectively. Each of these values exceed ground state of absorption cross-section ($\sigma_0 = 1.7 \times 10^{-17}$ for **3a** and 1.97×10^{-17} for **3b**) by factors of 5 and 3. These values are a very good indicator that RSA could be occurring for the Pcs.

Saturation fluence (F_{sat}) curves of **3a** and **3b** are compared by plotting transmittance (T) against the input fluence (I_0) (Fig. 8). The plots showed rapid decrease in transmittance as the input fluence increases. Similar observations ascribed to 2PA for organic compounds have been previously reported [60,61].

At I_0 values higher than 0.18 J cm^{-2}, more rapid decrease of transmittance for **3b** with respect to **3a** was observed which can be attributed to the difference in carbon chain-lengths of the alkynyl substituents on the peripheral positions of the Pcs. Thus, complex **3b** showed better NLO property than **3a** and this further corroborate our earlier result on its low fluorescence quantum yields and lifetimes in (Table 1) due to self-quenching by alkynyl moieties in **3a** than propagyl chain length of **3b**.

3.4.3. Limiting intensity (I_{lim})

Limiting intensity curves of the two alkynyl phthalocyanines (**3a** and **3b**) are presented in Fig. 9. An important parameter that has been reported in the literature to measure the optical limiting performance of materials is incident intensity threshold, (I_{lim}) which is defined as the input intensity at 50% linear transmittance [16]. Low value of I_{lim} is an indication of a good NLO response to the input intensity. From Table 2, complex **3b** has lower I_{lim} value hence exhibits larger optical limiting response than that of complex **3a**. In addition, values of I_{lim} obtained for both complexes were found to be among the lowest reported for phthalocyanines derivatives in recent literatures which ranged from 0.2 to 0.8 J cm^{-2}[13,15,22,62].

Another measure of effective nonlinear response of optical materials is excited to ground state absorption cross-sections ratio (k) which is defined as the ratio of σ_T to σ_0 [63]. For RSA, it implies that $\sigma_T > \sigma_0$ such that σ_T/σ_0 is greater than unity. The k values of 5.17 and 3.46 (Table 2) for complexes **3a** and **3b**, respectively were obtained. The k value observed for the complexes showed that the absorbance around the 532 nm region and 10 ns pulse radiation will predominantly be due to triplet–triplet absorption [22,37,63,64].

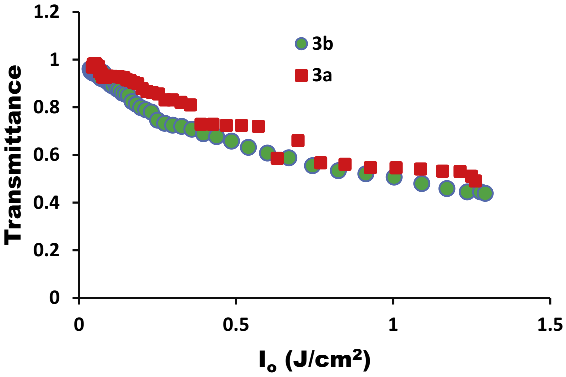

Fig. 8. Transmittance vs input fluence (I_0) curves for **3a** (red ■) and **3b** (green ●) in DMSO. Peak input intensity (I_{00}) ≈ 130 MW cm^{-2} for each sample. (Color online.)

3.4.4. Third-order nonlinear susceptibility ($I_m[\chi^{(3)}]$) and second-order hyperpolarizability (γ)

γ measures the interaction of incident photon with the permanent dipole moments of the alkynyl Pcs. Good optical limiting materials must have high absorbency as the intensity of the incident light is increased. Hence, the higher the γ values, the better the compounds are as optical limiters. Complex **3b** gave better values than **3a** at 3.19×10^{-32} and 2.7×10^{-32} esu, respectively, Table 2. $I_m[\chi^{(3)}]$ measures the fast response of a nonlinear optical material to the perturbation initiated by intense laser pulses. Estimated values for $I_m[\chi^{(3)}]$ and the two-photon absorption cross-sections (σ_2) for the two Pcs are high and consistent for organic molecules as nonlinear optical materials [15,22,62–64].

To show the merits and potentials of our molecules as nonlinear optical materials, the obtained values for $I_m[\chi^{(3)}]$, γ, k and β_2 in this work were compared with different phthalocyanines (In-phthalocyanines inclusive) that have been previously reported [65]. The values for $I_m[\chi^{(3)}]$ and γ reported in this work are on the high side for optical materials, while k and β_2 are within the range of values reported for the studied phthalocyanines. This suggests that our synthesized molecules have good prospects as optical limiters against laser radiation.

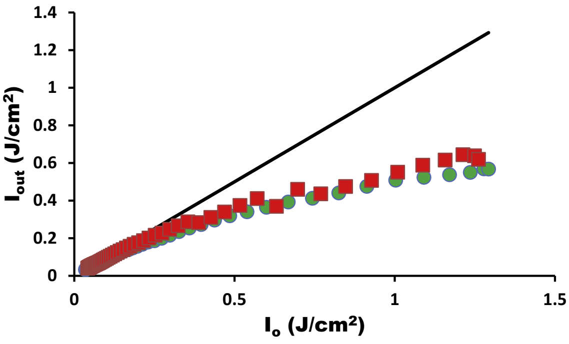

Fig. 9. Output fluence (I_{out}) vs input fluence (I_0) for complexes **3a** (■) and **3b** (●). The black solid line represents a case of linear transmission. Peak intensity (I_{00}) ≈ 130 MW cm^{-2} for each sample.

4. Conclusions

In summary, two novel tetra-alkynyl indium phthalocyanines have been synthesized and characterized. The two complexes showed high triplet quantum yields (close to unity). This further justified the high rate of intersystem crossing from excited singlet state to first excited triplet state. We also present our results on the nonlinear optical properties of the novel In-phthalocyanines with open aperture Z-scan studies at 532 nm, 10 ns pulses in dimethylsulfoxide. The results suggest that the nonlinear optical processes could be occurring *via* either sequential photon absorption (RSA) or a two-photon absorption mechanism for the studied In-phthalocyanines. Due to the fact that there was some uncertainty about which mechanism was responsible for the optical limiting, both were tested against the data. The analyses of the Z-scan data obtained did fit to a two-photon absorption mechanism, but the Pcs also possess the necessary excited state-ground state cross-section ratio to have RSA occur. Complex **3b** generally showed larger values of third-order susceptibility ($I_m[\chi^{(3)}]$) and second-order hyperpolarizability (γ), with an accompanying low value of incident intensity threshold (I_{lim}) compared to **3a**. Complex **3b** therefore exhibited better optical limiting behavior than **3a**. The results obtained in this work represented the first verification of the direct influence of the alkynyl moieties on the nonlinear optical properties of the indium phthalocyanines. Our studies suggest that these molecules can be tailored for potential applications in nonlinear optics by incorporating them into a thin film or polymer matrix.

Acknowledgements

This work was supported by the Department of Science and Technology (DST)/Nanotechnology (NIC) and National Research Foundation (NRF) of South Africa through DST/NRF South African Research Chairs Initiative for Professor of Medicinal Chemistry and Nanotechnology (UID = 62620) and Rhodes University.

References

[1] A.N. Cammidge, H. Gopee, Chem. Commun. (2002) 966

[2] M. Kimura, H. Ueki, K. Ohta, H. Shirai, N. Kobayashi, Langmuir 22 (2006) 5051.

[3] I. Okura, Photosensitization of Porphyrins and Phthalocyanines, Gordon and Breach Science Publishers, The Netherlands, Amsteldijk, 2001. pp. 151–213.

[4] R. Bonnet, Chemical Aspect of Photodynamic Therapy, Gordon and Breach, Amsterdam, 2000.

[5] M.J. Cook, N.B. McKeown, J.M. Simmons, A.J. Thomson, M.F. Daniel, K.J. Harrison, R.M. Richardson, S.J. Roser, J. Mater. Chem. 1 (1991) 121.

[6] F.H. Moser, A.L. Thomas, The Phthalocyanines: Manufacture and Applications, vol. 2, CRC Press, Boca Raton, Florida, 1983.

[7] M. Kimura, H. Ueki, K. Ohta, J. Chem. Eur. 10 (2004) 4954.

[8] J.A.A.W. Elemans, W.R. van Hameren, R.J.M. Nolte, A.E. Rowan, Adv Mater. 18 (2006) 1252.

[9] J. Mack, N. Kobayashi, Chem. Rev. 111 (2011) 281.

[10] G. de la Torre, P. Vazquez, F. Agullo-Lopez, T. Torres, Chem. Rev. 104 (2004) 3723.

[11] B.K. Mandal, B. Bihari, A.K. Sinha, M. Kamath, Appl. Phys. Lett. 66 (1995) 932.

[12] D. Dini, M. Hanack, in: K.M. Kadish, K.M. Smith, R. Guilard (Eds.), The Porphyrin Handbook: Physical Properties of Phthalocyanine based Materials, vol. 17, Academic Press, New York, 2003, p. 22.

[13] K. Sanusi, E.K. Amuhaya, T. Nyokong, J. Phys. Chem. C 118 (2014) 7057.

[14] J.S. Shirk, R.G.S. Pong, S.R. Flom, H. Heckmann, M. Hanack, J. Phys. Chem. A 104 (2000) 1438.

[15] R.S.S. Kumar, S.V. Rao, L. Giribabu, D.N. Rao, Chem. Phys. Lett. 447 (2007) 274.

[16] Y. Chen, L. Gao, M. Feng, L. Gu, N. He, J. Wang, Y. Araki, W.J. Blau, O. Ito, Mini-Rev. Org. Chem. 6 (2009) 55.

[17] P.K. Hegde, A.V. Adhikari, M.G. Manjunatha, P. Poornesh, G. Umesh, Opt. Mater. 31 (2009) 1000.

[18] F.E. Hernandez, S. Yang, E.W. Van Stryland, D.J. Hagan, Opt. Lett. 25 (2000) 1180.

[19] A. Iwase, C. Harnoode, Y.J. Kameda, J. Alloys Compd. 192 (1993) 280.

[20] C. Li, L. Zhang, M. Yang, Y. Wang, Phys. Rev. A 49 (1994) 1149.

[21] N.B. McKeown, in: K.M. Kadish, K.M. Smith, R. Guilard (Eds.), The Porphyrin Handbook: Physical Properties of Phthalocyanine based Materials, Academic Press, New York, 2003.

[22] S.O. Sanusi, E. Antunes, T. Nyokong, J. Porphyr. Phthalocyan. 17 (2013) 920.

[23] D.K. Modibane, T. Nyokong, Polyhedron 28 (2009) 1475.

[24] J. Britton, C. Litwinski, M. Durmus, V. Chauke, T. Nyokong, J. Porphyr. Phthalocyan. 15 (2011) 1239.

[25] X.F. Zhang, X. Li, L. Niu, L. Sun, L. Liu, J. Fluoresc. 19 (2009) 947.

[26] M. Hanack, D. Dini, M. Barthel, S. Vagin, Chem. Rec. 2 (2002) 129.

[27] M. Yamaji, H. Maeda, Y. Nanai, K. Mizuno, Intern. Scholar. Res. Network: Phys. Chem. 103817 (2012), http://dx.doi.org/10.5402/2012/103817. 7 p..

[28] E.M. García-Frutos, S.M. O'Flaherty, E.M. Maya, G. de la Torre, W. Blau, P. Vázqueza, T. Torres, J. Mater. Chem. 13 (2003) 749.

[29] D. Dini, M. Barthel, M. Hanack, Eur. J. Org. Chem. (2001) 3759

[30] F. Kajzar, J. Messier, C. Rosilio, J. Appl. Phys (1986) 3040.

[31] S. Fery-Forgues, D. Lavabre, J. Chem. Educ. 76 (1999) 1260.

[32] T.H. Tran-Thi, C. Desforge, C. Thiec, J. Phys. Chem. 93 (1989) 1226.

[33] A. Ogunsipe, J.Y. Chen, T. Nyokong, New J. Chem. 7 (2004) 822.

[34] M. Sheik-Bahae, A.A. Said, E.W. Stryland, Opt. Lett. 14 (1989) 955.

[35] M. Sheik-Bahae, A.A. Said, T. Wei, D.J. Hagan, E.W. Van Stryland, IEEE J. Quantum Electron. 26 (1990) 760.

[36] J.E. Ehrlich, X.L. Wu, I.Y.S. Lee, Z.Y. Hu, H. Röckel, S.R. Marder, J.W. Perry, J. Opt. Lett. 22 (1997) 1843.

[37] Y. Chen, M. Hanack, Y. Araki, O. Ito, Chem. Soc. Rev. 34 (2005) 517.

[38] C.C. Leznoff, S.B. Bohdan, Can. J. Chem. 79 (2001) 878.

[39] D.S. Terekhov, K.J.M. Nolan, C.R. McArthur, C.C. Leznoff, J. Org. Chem. 61 (1996) 3034.

[40] G. Bottari, D.D. Díaz, T. Torres, J. Porphyr. Phthalocyan. 10 (2006) 1083.

[41] Y. Yılmaz, J. Mack, M. Sönmez, T. Nyokong, J. Porphyr. Phthalocyan. 18 (2014) 251.

[42] İ. Özceşmeci, A. Gelir, A. Gül, J. Luminescence 147 (2004) 141.

[43] M. Durmuş, S. Yeşilot, V. Ahsen, New J. Chem. 30 (2006) 675.

[44] A.Y. Tolbin, V.E. Pushkarev, G.F. Nikitin, L.G. Tomilova, Tetrahedron Lett. 69 (2009) 4848.

[45] H. Dinçer, H. Mert, B.N. Şen, A. Dağ, S. Bayraktar, Dyes Pigments 98 (2013) 246.

[46] S.Y. Al-Raqa, Dyes Pigments 77 (2008) 259.

[47] M. Durmus, T. Nyokong, Photochem. Photobiol. Sci. 6 (2007) 659.

[48] T. Nyokong, H. Isago, *J.* Phthalocyanines Porphyrins 8 (2004) 1083.

[49] E. Glimsdal, M. Carlsson, T. Kindahl, M. Lindgren, C. Lopes, B. Eliasson, J. Phys. Chem. A114 (2010) 3431.

[50] A. Lyubimtsev, Z. Iqbala, G. Cruciusa, S. Syrbub, E.S. Taraymovich, T. Ziegler, M. Hanack, J. Porphyr. Phthalocyan. 15 (2011) 39.

[51] J.A. Lacey, D. Phillips, Photochem. Photobiol. *Sci.* 1 (2002) 378.

[52] K. Ishii, N. Kobayashi, in: K.M. Kadish, K.M. Smith, R. Guilard (Eds.), The Porphyrin Handbook, vol. 16, Elsevier, 2003 (Chapter 1).

[53] S.J. Mathews, S.C. Kumar, L. Giribabu, S.V. Rao, Opt. Commun. 280 (2007) 206.

[54] R.L. Sutherland, in: Marcel Dekker, (Ed.), Handbook of Nonlinear Optics, New York, NY, second ed. 2003 (revised and expanded).

[55] M. Hanack, T. Schneider, M. Barthel, J.S. Shirk, S.R. Flom, R.G.S. Pong, Coord. Chem. Rev. 219 (2001) 235.

[56] M. Hercher, Appl. Opt. 9 (1967) 947.

[57] H.S. Nalwa, J.S. Shirk, in: C.C. Cliznoff, A.B.P. Lever (Eds.), Phthalocyanines: Properties and Applications, vol. 4, VCH, New York, 1996.

[58] L.W. Tutt, T.F. Boggess, Prog. Quantum Electron. 17 (1993) 299.

[59] P.L. Chen, I.V. Tomov, A.S. Dvornikov, M. Nakashima, J.F. Roach, D.M. Alabran, P.M. Rentzepis, J. Phys. Chem. 100 (1996) 17507.

[60] T. Pritchett, Models for saturable and reverse saturable absorption in materials for optical limiting, in: Sensors and Electron Devices Directorate, ARL, 2002, p. 1.

[61] S.H. Guang, R. Gvishi, P.N. Prasad, B.A. Reinhardt, Opt. Commun. 117 (1995) 133.

[62] M. Yuksek, A. Elmali, M. Durmus, H.G. Yaglioglu, H. Unver, T. Nyokong, *J.* Opt. 12 (2010) 1.

[63] A. Auger, W.J. Blau, P.M. Burnham, I. Chambrier, M.J. Cook, B. Isare, F. Nekelsona, S.M. O'Flaherty, J. Mater. Chem. 13 (2003) 1042.

[64] J. Wang, M. Sheik-Bahae, A.A. Said, D.J. Hagan, E.W. Van Stryland, J. Opt. Soc. Am. B 11 (1994) 1009.

[65] S.M. O'Flaherty, S.V. Hold, M.J. Cook, T. Torres, Y. Chen, M. Hanack, W.J. Blau, Adv. Mater. 15 (2003) 19.